

# When Poor Light-Emitting Spiro Compounds in Solution Turn into Emissive Pure Layers in Organic Light-Emitting Diodes: The Key Role of Phosphine Substituents

Pauline Tourneur, Fabien Lucas, Clément Brouillac, Cassandre Quinton, Roberto Lazzaroni, Yoann Olivier, Pascal Viville, Cyril Poriel,\* and Jérôme Cornil\*

Spiro compounds are widely used as host matrices in organic light-emitting diodes (OLEDs). Here, inspired by the recent developments in thermally activated delayed fluorescence (TADF) materials, the potential as a light emitter of two spiro-configured organic semi-conductors is investigated, constructed by the association of quinolinophenothiazine (QPTZ) or indoloacridine (IA) as the electron-rich fragment and diphenylphosphine oxide fluorene as the electron-poor fragment. By comparison with structural analogues lacking phosphine oxides, the crucial role played by these electron-accepting substituents not only on the photo-physical properties but also on the device performances is evidenced. Despite a very low quantum yield in solution, these two compounds unexpectedly display good emission properties when incorporated as a pure layer in OLEDs, thus highlighting the role of intermolecular effects.

## 1. Introduction

The field of organic light-emitting diodes (OLEDs) has made fantastic progress in the past 20 years and is now a viable technology.<sup>[1]</sup> All these efforts have led to the development of three main families of emitting materials based on different photo-physical concepts: fluorescence (generation I),<sup>[2–4]</sup> phosphorescence (generation II),<sup>[5–11]</sup> and thermally activated delayed fluorescence (TADF, generation III).<sup>[12,13]</sup> Nowadays, generation II is the most mature although generation III has the advantage to avoid the use of organo-metallic complexes to recover both singlet and triplet excited states. Moreover, the next generations of emitting materials such


as those based on hyperfluorescence<sup>[14]</sup> are fast-emerging so even better devices are expected in the near future.<sup>[1]</sup> Studying new approaches to molecular design to uncover new ways of producing light emission is an important topic in the field, which has notably led to the fast deployment of the TADF concept.<sup>[12]</sup> To ease the upscaling process, another desirable feature is to simplify as much as possible the OLED architecture<sup>[15]</sup> by reducing the number of layers of the device (with fluorescent,<sup>[2]</sup> phosphorescent,<sup>[9]</sup> or TADF<sup>[15]</sup> materials) or by avoiding the use of mixed layers.<sup>[16]</sup> In a recent work, we have unraveled the intriguing spectroscopic properties of a spiro-configured compound (named SPA-F(POPh<sub>2</sub>)<sub>2</sub>) built on the association of a phenylacridine and a diphenylphosphine oxide fluorene.<sup>[16]</sup> Such a donor-spiro-acceptor molecular architecture has been widely used to design high-efficiency host matrices in phosphorescent OLEDs<sup>[17–19]</sup> and has been considered less often as a potential emitter in spite of the donor-acceptor character typically involved in TADF emission.<sup>[20]</sup> Moreover, spiro compounds are known to exhibit good luminescence properties in the solid state owing to their cumbersome architecture limiting the impact of detrimental intermolecular interactions.<sup>[21]</sup> It turned out that SPA-F(POPh<sub>2</sub>)<sub>2</sub> not only displays a very unusual dual emission in solution and thin solid films but also generates an unexpected white light emission when incorporated as a pure layer (i.e., without any host) in OLEDs. This has been rationalized by the fact that intermolecular charge-transfer states (i.e., exciplexes) between the donor branch of one molecule and the acceptor branch of another significantly contribute to the emission.

P. Tourneur, R. Lazzaroni, J. Cornil  
Laboratory for Chemistry of Novel Materials  
University of Mons  
7000 Mons, Belgium  
E-mail: jerome.cornil@umons.ac.be

F. Lucas, C. Brouillac, C. Quinton, C. Poriel  
ISCR-UMR 6226  
Université de Rennes 1  
CNRS  
35700 Rennes, France  
E-mail: cyril.poriel@univ-rennes1.fr

Y. Olivier  
Laboratory for Computational Modeling of Functional Materials  
Université de Namur  
5000 Namur, Belgium

P. Viville  
Materia Nova  
Materials R&D Center  
7000 Mons, Belgium

 The ORCID identification number(s) for the author(s) of this article can be found under <https://doi.org/10.1002/adpr.202200124>.

© 2022 The Authors. Advanced Photonics Research published by Wiley-VCH GmbH. This is an open access article under the terms of the Creative Commons Attribution License, which permits use, distribution and reproduction in any medium, provided the original work is properly cited.

DOI: 10.1002/adpr.202200124

It is well established that exciplex formation does contribute to light emission in OLEDs<sup>[22,23]</sup> but they are most often generated in blends rather than in a pure layer, as is the case here. Nevertheless, the exact role played by the phosphine oxides in promoting the intriguing properties of SPA-F(POPh<sub>2</sub>)<sub>2</sub> remains unclear. The observed behavior cannot be associated with aggregation-induced effects (AIE), which are typically triggered by conformational changes when going from the solution to the solid phase<sup>[24]</sup> since spiro compounds display very rigid structures, preventing pronounced torsional fluctuations around the spiro carbon.

In this work, following a similar design approach, we extend our work to a new series of donor-spiro-acceptor compounds built on two donor units, namely quinolinophenothiazine in SQPTZ-F(POPh<sub>2</sub>)<sub>2</sub> (whose synthesis is reported elsewhere<sup>[25]</sup>) and indoloacridine in SIA-F(POPh<sub>2</sub>)<sub>2</sub> both coupled to the 2,7-bis(diphenylphosphineoxide)-fluorene fragment as an electron-accepting unit. Quinolinophenothiazine (QPTZ)<sup>[26,27]</sup> and indoloacridine (IA)<sup>[28–31]</sup> can be seen as a rigidified phenylacridine fragment and have been much less studied than their parent counterpart. To shed light on the impact of the phosphine oxide units, similar molecules without these fragments were also investigated (SQPTZ-F<sup>[26]</sup> and SIA-F<sup>[28]</sup>); the chemical structures of the compounds are reported in Figure 1. This comparison shows that the phosphine oxides contribute systematically to significantly improve the device performances compared to the unsubstituted analogues. In particular, SIA-F(POPh<sub>2</sub>)<sub>2</sub> gives strong evidences that exciplexes formed by the donor branch of one molecule and the acceptor branch of another are responsible for electroluminescence signal.

## 2. Results and Discussion

We have first explored the electronic and optical properties of isolated SQPTZ-F versus SQPTZ-F(POPh<sub>2</sub>)<sub>2</sub> at the (time-dependent) density functional theory—(TD)-DFT—level. For the sake of coherence with our previous works,<sup>[32]</sup> these calculations have been performed using the hybrid PBE0 functional and a 6-31G\*\* basis set; the TD-DFT calculations have been performed within the Tamm–Dancoff approximation.<sup>[33–35]</sup> For both molecules, there is a clear spatial separation between the highest occupied molecular orbital (HOMO) and lowest unoccupied molecular orbital (LUMO) orbitals, with the HOMO level localized on the electron-rich QPTZ core and the LUMO on the fluorene unit in SQPTZ-F and the electron-poor diphenylphosphine oxide fluorene in SQPTZ-F(POPh<sub>2</sub>)<sub>2</sub> (Figure 2a). The introduction of the phosphine oxide substituents stabilizes the LUMO level by 0.77 eV while the HOMO energy is hardly affected, as expected from its localization in the electron-rich unit. This translates in turn to a red shift by 0.70 eV of the lowest S<sub>1</sub> excited state, which is mostly described by a HOMO to LUMO transition. In both cases, the lowest excited state is weakly optically coupled to the ground state (with an oscillator strength of 2.10<sup>−4</sup> for SQPTZ-F and 1.10<sup>−3</sup> for SQPTZ-F(POPh<sub>2</sub>)<sub>2</sub>). This is primarily driven by the fact that the donor and acceptor moieties are orthogonal to each other, around the spiro carbon; such a situation should lead to low fluorescence quantum yield in solution (see the following). The detachment/attachment formalism has

been used to visualize the electronic density removed in the ground state upon excitation (detachment) and the way it is rearranged in the excited state (attachment) (see typical plots in the gas phase in Figure 2b).<sup>[36]</sup> The charge-transfer (CT) character in an excited state can be evaluated by Φ<sub>S</sub> reflecting the overlap between the electron and hole density<sup>[33,37,38]</sup> (Φ<sub>S</sub> = 1 for a purely localized character, and 0 for a pure CT excitation). Φ<sub>S</sub> is determined to be 0.32 in SQPTZ-F (i.e., very similar to the value computed for 2CzPN<sup>[39]</sup>) and 0.16 in SQPTZ-F(POPh<sub>2</sub>)<sub>2</sub>, showing the strong CT nature of this state, further reinforced by the introduction of the phosphine units in the latter compound.

Regarding the triplet manifold, there are five triplet states below S<sub>1</sub> in SQPTZ-F; the energy difference between S<sub>1</sub> and T<sub>1</sub> (ΔE<sub>ST</sub>) amounts to 0.44 eV and is expected to be highly detrimental for a TADF process. In contrast, this energy gap is reduced to 0.03 eV for SQPTZ-F(POPh<sub>2</sub>)<sub>2</sub>, a beneficial feature for TADF; this matches very well the experimental values of 0.43 and −0.08 eV, respectively (see Figure S17 and S18, Supporting Information). When considering SIA-F versus SIA-F(POPh<sub>2</sub>)<sub>2</sub>, Figure 1, the main difference is the accidental quasi degeneracy of the LUMO level of the donor and acceptor branches in SIA-F, leading to a LUMO delocalized over the whole molecule. As a result, the oscillator strength of the lowest excited state is significantly larger (6.10<sup>−2</sup>) and Φ<sub>S</sub> = 0.6. ΔE<sub>ST</sub> is large in the two compounds (0.62 eV in SIA-F and 0.38 eV in SIA-F(POPh<sub>2</sub>)<sub>2</sub>); this compares remarkably well with the corresponding experimental value of 0.60 and 0.41 eV (see Figure S15 and S16, Supporting Information).

We have next compared the experimental absorption spectra in dichloromethane and the corresponding theoretical spectra of SQPTZ-F(POPh<sub>2</sub>)<sub>2</sub> and SQPTZ-F (Figure 3, top). According to the calculations, the S<sub>1</sub> state is not observed in the spectra due to its very low oscillator strength. Actually, the lowest absorption band observed in the experimental spectra originates from the S<sub>2</sub> and S<sub>3</sub> states in SQPTZ-F and S<sub>2</sub> state in SQPTZ-F(POPh<sub>2</sub>)<sub>2</sub>. A noticeable difference in SIA-F is that the S<sub>1</sub> state is clearly distinguished due to its pronounced oscillator strength, as discussed earlier.

In emission spectroscopy (Figure 4), the difference between SQPTZ-F(POPh<sub>2</sub>)<sub>2</sub> and SQPTZ-F becomes significant, showing the strong impact of the phosphine oxides. Indeed, the emission of SQPTZ-F is peaking at 419 nm in dichloromethane whereas that of SQPTZ-F(POPh<sub>2</sub>)<sub>2</sub> is strongly red-shifted down to 540 nm (red shift of ≈0.6 eV, very comparable to the theoretical results); the intrinsic character of these observations is supported by the excitation spectra reported in Figure S19, Supporting Information. In addition, there is a significant solvatochromic shift in the case of SQPTZ-F(POPh<sub>2</sub>)<sub>2</sub> (from 452 nm in cyclohexane to 591 nm in MeOH, see Figure S1, Supporting Information) but a very small shift in the case of SQPTZ-F (<5 nm). This reflects the more pronounced charge transfer character of the former compound, as further evidenced by the smaller value of the Φ<sub>S</sub> parameter. In air, the fluorescence decay curve of SQPTZ-F(POPh<sub>2</sub>)<sub>2</sub> displays one single lifetime of 15.9 ns (see Figure S11, S12, Supporting Information), whereas SQPTZ-F displays a very short single lifetime <1 ns (see Figure S6, Supporting Information). In argon, the decay emission profile of the main band (at 497 nm in toluene) of SQPTZ-F(POPh<sub>2</sub>)<sub>2</sub> displays a long tail extending up to the

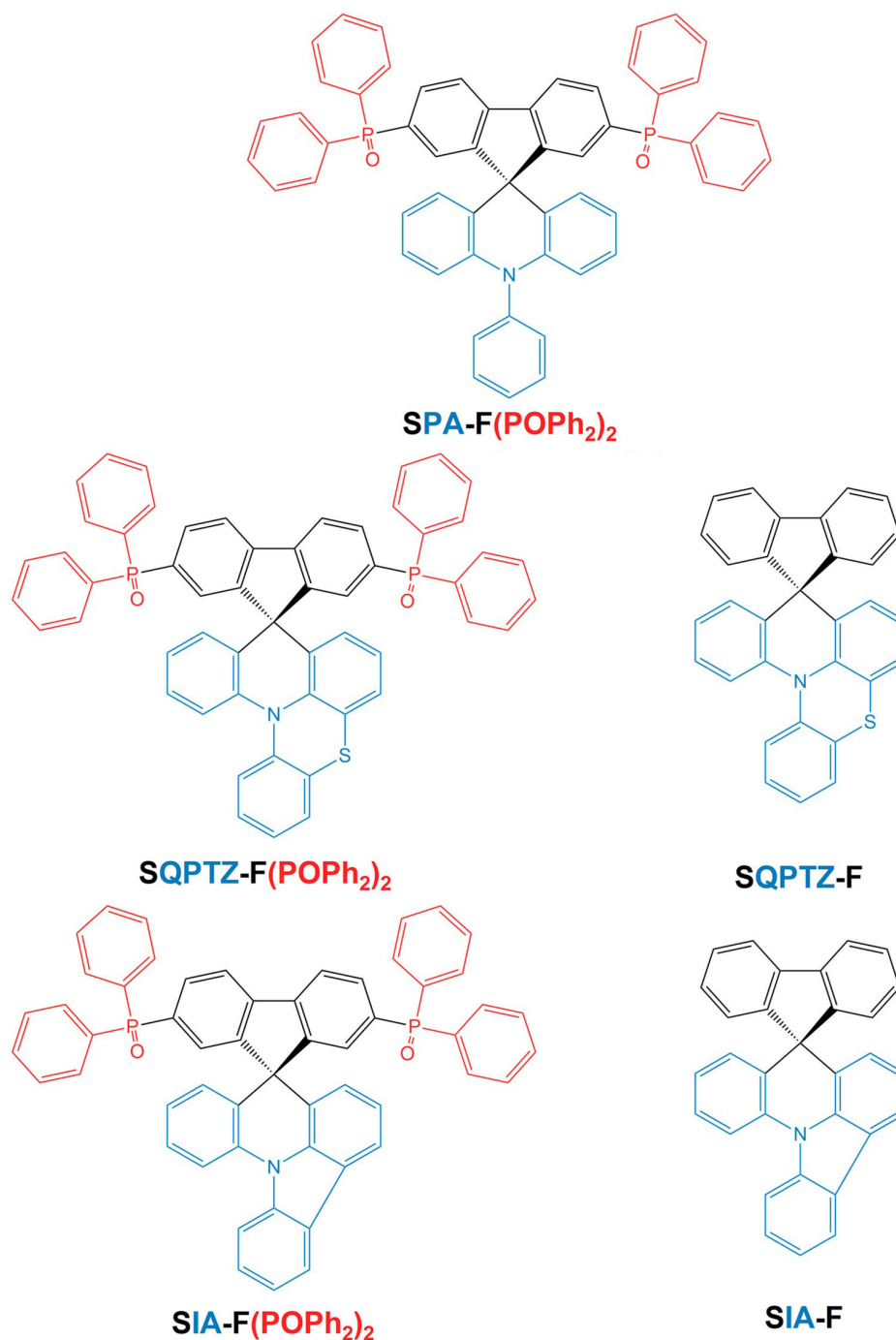


**Figure 1.** Molecular structures under study in this work and of SPA-F(POPh<sub>2</sub>)<sub>2</sub> investigated in Ref. [16].

microsecond timescale (75  $\mu$ s), suggesting a delayed fluorescence mechanism (see Figure S14, Supporting Information). SQPTZ-F does not display any delayed fluorescence (see Figure S5–S7, Supporting Information), showing again the strong impact of the phosphine oxides on the photo-physical processes.

The behavior of the SIA-F(POPh<sub>2</sub>)<sub>2</sub>/SIA-F couple is similar to that of SQPTZ-F(POPh<sub>2</sub>)<sub>2</sub>/SQPTZ-F in terms of solvatochromic shift (significant shift, >100 nm for SIA-F(POPh<sub>2</sub>)<sub>2</sub> and a very

small shift, 10 nm, for SIA-F,<sup>[27]</sup> see Figure S1, Supporting Information) and is somewhat different in time-resolved fluorescence. In air, a single lifetime is measured: 5.2 ns for SIA-F(POPh<sub>2</sub>)<sub>2</sub> and 5.1 ns for SIA-F without delayed fluorescence for both (Figure S2–S4, S8–S10, Supporting Information). This highlights how the nature of the donor unit can modify the photophysical processes and particularly the TADF process. These behaviors are fully consistent with the calculations

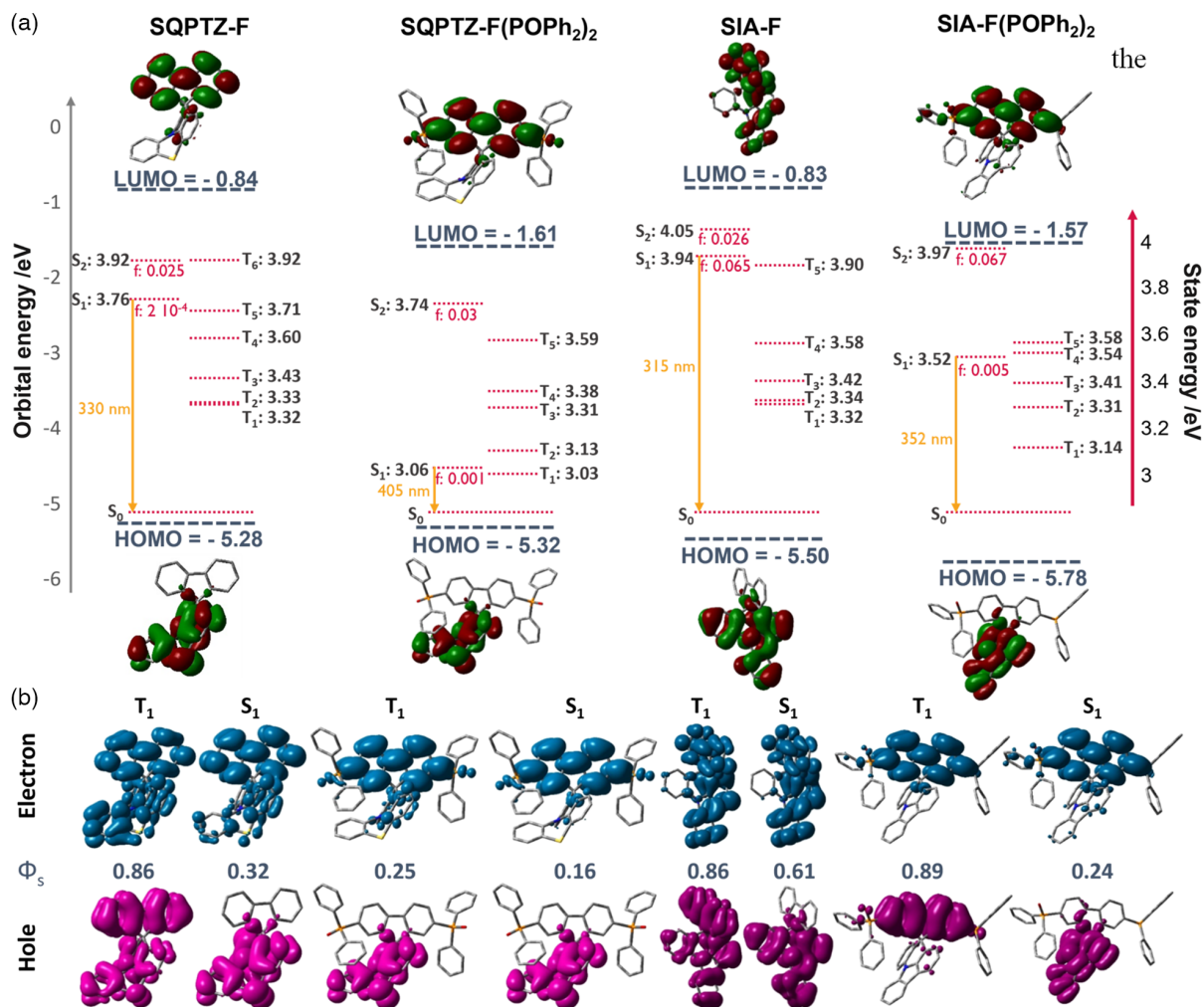


**Figure 2.** a) Shape and energy levels of the HOMO and LUMO of SQPTZ-F/SQPTZ-F(POPh<sub>2</sub>)<sub>2</sub> and SIA-F/SIA-F(POPh<sub>2</sub>)<sub>2</sub> in their ground state geometry and energies of the lowest excited states together with the corresponding oscillator strength; b) Representations of hole detachment and electron attachment densities for SQPTZ-F, SQPTZ-F(POPh<sub>2</sub>)<sub>2</sub>, SIA-F and SIA-F(POPh<sub>2</sub>)<sub>2</sub> in the gas phase.

showing that SQPTZ-F(POPh<sub>2</sub>)<sub>2</sub> is the only compound to exhibit a small  $\Delta E_{ST}$  value ( $<0.2$  eV), thus promoting a small energy barrier for Reverse InterSystem Crossing (RISC) required for efficient TADF processes.<sup>[38]</sup> The different lifetimes obtained in the argon atmosphere are summarized in Table S2, Supporting Information.

The fluorescence quantum yields of both SQPTZ-F(POPh<sub>2</sub>)<sub>2</sub> and SIA-F(POPh<sub>2</sub>)<sub>2</sub> are measured to be below 1% in solution in cyclohexane, in contrast to many TADF molecules that are luminescent in solution.<sup>[40]</sup> This is expected in view of the very low oscillator strength arising from the spatial separation of the electron-rich and the electron-poor fragments, which promotes a vanishingly small transition dipole moment between the S<sub>1</sub> and S<sub>0</sub> states; moreover, the strong rigidity of the backbone prevents the modulation of the optical properties via geometric distortions involving changes in torsion angles.<sup>[39]</sup> For the same reason, the quantum yield of the model compound SQPTZ-F is also recorded below 1%. SIA-F displays a different behavior with a quantum yield significantly increased to ca 14%, due to the

higher oscillator strength of the lowest excited state (see above). The thermally evaporated thin solid film fluorescence spectra are very similar to those in solution (Figure 4), indicating that the fluorophores are weakly interacting in the solid state due to the spiro arrangement. The shifts are mostly attributed to changes in the polarity of the medium when going from dichloromethane to the thin film in view of the large solvatochromism of these compounds. We note for SQPTZ-F(POPh<sub>2</sub>)<sub>2</sub> the appearance of a weak emission between 350 and 400 nm. This unexpected feature has already been observed with the structurally related analogue SPA-F(POPh<sub>2</sub>)<sub>2</sub>, bearing a phenylacridine unit instead of a QPTZ unit and has been assigned to an emission occurring from a higher lying excited state.<sup>[16]</sup> The phosphine oxide units appear to trigger this peculiar emission since SIA-F(POPh<sub>2</sub>)<sub>2</sub> also displays a similar low-intensity band while it is absent in SQPTZ-F and SIA-F. It is worth stressing that the emission spectra in thin solid films of SQPTZ-F(POPh<sub>2</sub>)<sub>2</sub> and SIA-F(POPh<sub>2</sub>)<sub>2</sub> also exhibit a tail in emission at lower energy compared to the emission in solution

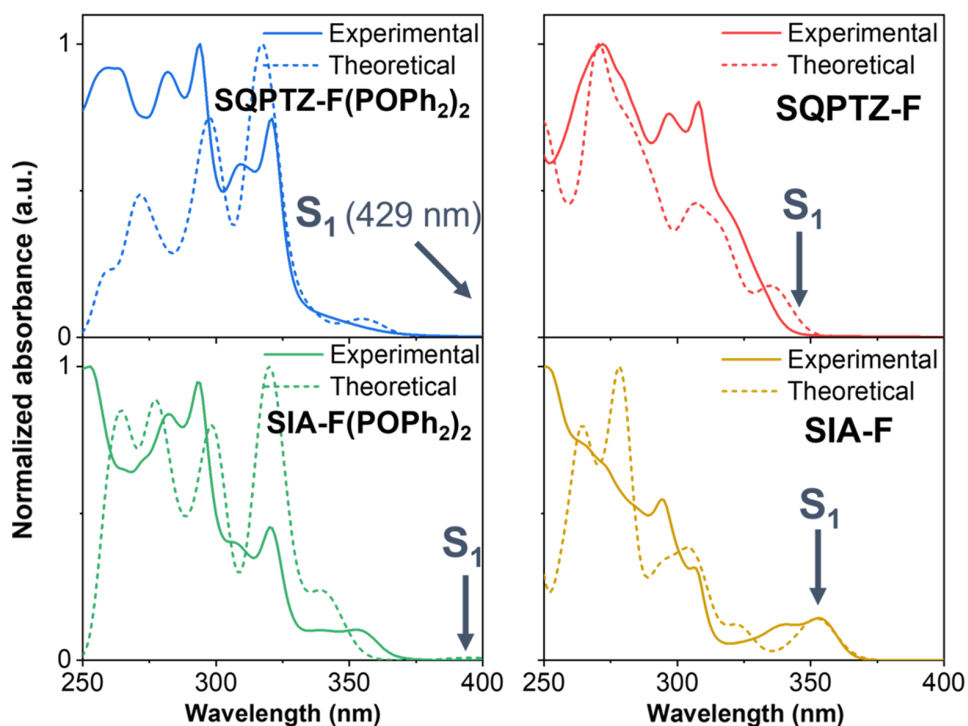


**Figure 3.** Top. Normalized experimental absorption spectra in dichloromethane and time-dependent density functional theory (TD-DFT) simulated spectra in the same solvent for **SQPTZ-F(POPh<sub>2</sub>)<sub>2</sub>** (Left) and **SQPTZ-F** (Right). The solvent effects have been accounted for in the simulations via the polarizable continuum model (PCM). The theoretical spectra have been further red-shifted by  $\approx 0.4$  eV to best match the experimental absorption. Bottom: corresponding spectra for **SIA-F(POPh<sub>2</sub>)<sub>2</sub>** (left) and **SIA-F** (right).

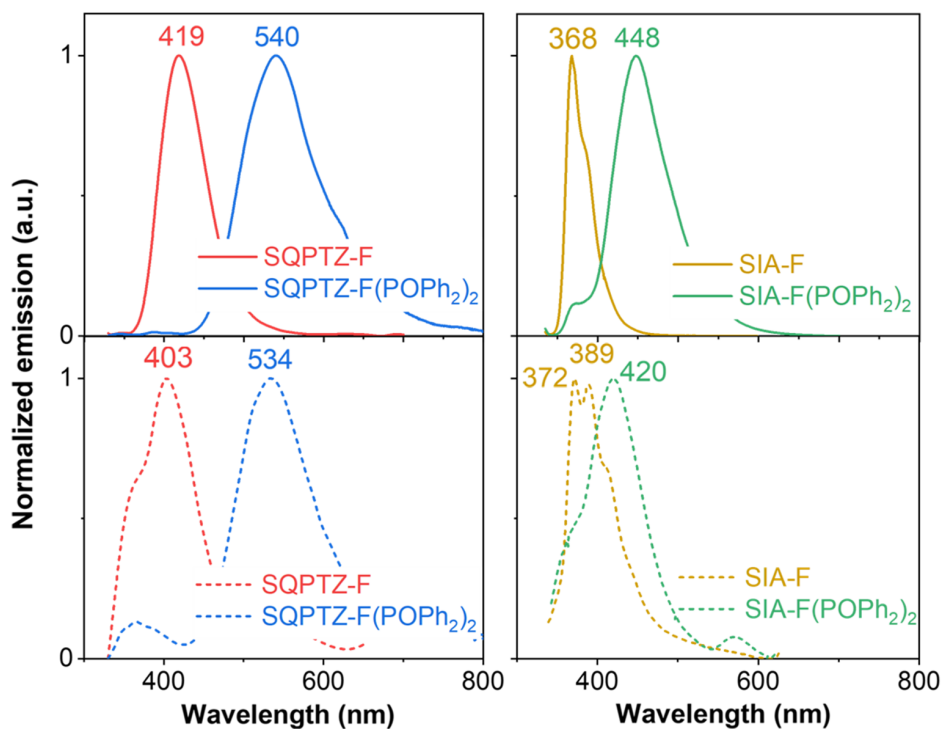


**Figure 4.** Normalized emission spectra in dichloromethane (Top) and as evaporated thin-films (bottom) for **SQPTZ-F(POPh<sub>2</sub>)<sub>2</sub>** and **SQPTZ-F** (Left,  $\lambda_{\text{exc}} = 310$  nm) and **SIA-F** and **SIA-F(POPh<sub>2</sub>)<sub>2</sub>** (Right,  $\lambda_{\text{exc}} = 320$  nm).

(Figure 4). We attribute this feature to the formation of intermolecular charge-transfer states (i.e., exciplexes) exploiting the donor branch of one molecule and the acceptor branch of another closely lying molecule. The red-shift of this band compared to the lowest intramolecular emitting state can be rationalized by a larger electron–hole separation in the exciplex compared to that in the charge-transfer  $S_1$  state of the individual compounds, promoting larger electronic polarization effects in the medium, and hence a larger stabilization of the exciplex CT energy.<sup>[41]</sup> The energy separation between these two bands (1.07 eV for **SQPTZ-F(POPh<sub>2</sub>)<sub>2</sub>** and 0.78 eV for **SIA-F(POPh<sub>2</sub>)<sub>2</sub>**) appears to be too large to be associated with aggregation effects (i.e., exciton delocalization), especially for spiro-compounds which are not prone to aggregation.<sup>[21]</sup> The quantum yields have been determined in thin films, see Table S1, Supporting Information. The quantum yield of **SQPTZ-F(POPh<sub>2</sub>)<sub>2</sub>** remains small though slightly increased from below 1% in solution to 3% in thin film. This behavior is not observed for the other fluorophores (**SIA-F(POPh<sub>2</sub>)<sub>2</sub>**, **SIA-F**, and **SQPTZ-F**, see values in Table S1, Supporting Information).

These compounds have been finally used under the form of a pure emitting layer (EML) in bottom-emitting OLEDs (ITO/ $\alpha$ -NPD (25 nm)/mCP (5 nm)/Emitter (20 nm)/DPEPO (5 nm)/TPBi (25 nm)/LiF (1 nm)/Al (100 nm)), see Figure S30, Supporting Information. A detailed protocol for the fabrication of the devices is provided in the Supporting Information. The electroluminescence signal is very weak for both **SIA-F** and **SQPTZ-F** and could not be easily separated from the background noise. Strikingly and despite a very low quantum yield (see above), the OLEDs based on **SQPTZ-F(POPh<sub>2</sub>)<sub>2</sub>** generate green light with CIE chromatic coordinates of (0.35; 0.54, Figure S31, Supporting Information), pointing again to the strong influence of the phosphine oxides. The electroluminescence spectrum is centered at 534 nm (Figure 5, left) and is very similar to the fluorescence obtained from thermally sublimed thin films, demonstrating the stability of the emitter in harsh OLED conditions. This good match further suggests that intramolecular CT states are at the origin of the electroluminescence signal since the weak feature associated with exciplexes does not contribute much to the EL spectrum; this implies that the generated intramolecular

CT states do not readily decay into exciplexes requiring possibly specific orientations of adjacent molecules to be generated. Interestingly, the emission at 375 nm is not observed in the electroluminescence spectrum, in consistent with the fact that the thermalized injected electrons and holes cannot recombine into a high-lying excited state(s).

The devices based on a pure layer of **SQPTZ-F(POPh<sub>2</sub>)<sub>2</sub>** present surprisingly good characteristics without device optimization, especially considering its very low quantum yield in solution, with a low turn-on voltage ( $V_{ON}$ ) of 5 V and a maximum EQE of 1.65% (averaged at  $1.29 \pm 0.37\%$  over 5 devices, see Figure S32, S33, Supporting Information), pointing not only to an efficient charge injection within the device but also to a good charge recombination. These performances cannot be readily compared with the values most often reported in the literature at low current density and low surface area since they are obtained here for relatively large areas (from 0.21 to 0.6 cm<sup>2</sup>) and for a current density of  $\approx 15/20$  mA cm<sup>-2</sup> accounting for the roll-off of the device efficiency with increasing current density. For sake of illustration, early devices based on the TADF emitter **2CzPN** yield an EQE of around 3% for a current density of  $\approx 10$  mA cm<sup>-2</sup>.<sup>[40]</sup>

These devices exhibit a maximum current efficiency of 5 Cd A<sup>-1</sup> at 5 mA cm<sup>-2</sup> and a brightness of 700 at 35 mA cm<sup>-2</sup> (see Figure S33, Supporting Information); the evolution of the brightness as a function of the applied bias is displayed in Figure 6. Since the hole-transporting mCP layer is known to be fluorescent, though more in the blue region (maximum of the emission around 400 nm), we have also fabricated similar devices without the mCP layer between  $\alpha$ -NPD and the emitter; when doing so, we have adjusted the thickness of the emissive layer to 25 nm to keep the same device cavity.

These devices do not present any major difference with respect to the previous ones (see Figure S34, Supporting Information): green light with CIE chromatic coordinates of (0.33; 0.53) is also generated. An EQE of  $(0.96 \pm 0.26)\%$  (averaged on 12 devices) at 10 mA cm<sup>-2</sup> as well as a higher maximum brightness of 1000 cd m<sup>-2</sup> for a higher current density of 75 mA cm<sup>-2</sup> have been recorded. These results clearly point out that the charge recombines in the **SQPTZ-F(POPh<sub>2</sub>)<sub>2</sub>** emissive

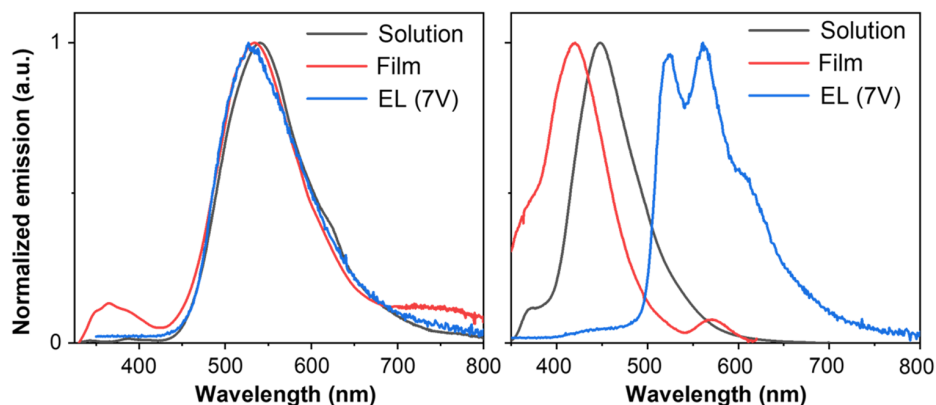


**Figure 5.** Comparison of the photoluminescence spectra ( $\lambda_{exc} = 310$  nm for **SQPTZ-F(POPh<sub>2</sub>)<sub>2</sub>** and  $\lambda_{exc} = 320$  nm for **SIA-F(POPh<sub>2</sub>)<sub>2</sub>**) in dichloromethane (black curves) and in films deposited by vacuum thermal sublimation (red curves) versus the electroluminescence spectrum recorded at 7 V (blue curves) for **SQPTZ-F(POPh<sub>2</sub>)<sub>2</sub>** (left) and **SIA-F(POPh<sub>2</sub>)<sub>2</sub>** (right).

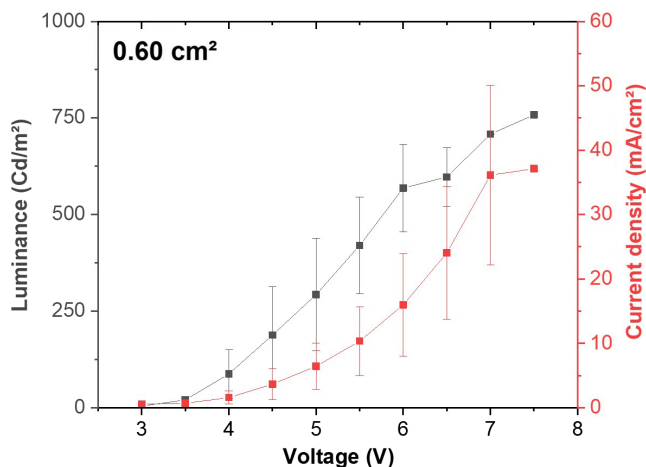


**Figure 6.** Luminance and current density as a function of the applied bias for SQPTZ-F(POPh<sub>2</sub>)<sub>2</sub>, as averaged over three devices with a surface area of 0.60 cm<sup>2</sup>.

layer and that the mCP layer does not affect the color rendering index and the EQE. Confirmation of the key role played by the phosphine oxide was obtained with SIA-F(POPh<sub>2</sub>), for which an electroluminescence signal is also observed with an EQE of (0.63 ± 0.09)% (averaged on 9 devices), see Figure S35, Supporting Information. The electroluminescence is here red-shifted by ≈0.6 eV compared to the main emission band in solution and in thin films. The emission energy range matches very well that of the tail observed in the thin film spectra, thus suggesting unambiguously that exciplexes are here responsible for the light emission. The high resolution (i.e., vibronic structure) seen in the exciplex spectrum is rather unexpected in view of the typically broad and unresolved bands associated with exciplex emission processes. We speculate that this could be rationalized by the progressive thermalization of the charge carriers into the most stable electronic levels while migrating across the organic layer and with the fact that only specific relative positions of two adjacent molecules yield exciplexes, thus limiting the extent of the structural and energetic disorder.

### 3. Conclusion

The present findings clearly go against the mainstream in the field of OLED technology since we are using an emitting layer without a host matrix and based on a poorly fluorescent compound. Since this peculiar behavior is not observed for the unsubstituted compounds, it turns out that the phosphine groups play a pivotal role in dictating the observed properties. Our results also suggest that exciplexes triggered by the introduction of phosphine units participate in the light emission in SIA-F(POPh<sub>2</sub>). This rather unexpected phenomenon calls for transient absorption spectroscopy measurements to gain a deeper insight into the photophysical processes.<sup>[42]</sup> Nevertheless, it is not unlikely that the excited-state kinetics is different when emitting species are generated by the decay of a higher lying excited state (since S<sub>1</sub> is optically forbidden) with a limited diffusion process of the excitons in the thin films versus the

recombination of free charge carriers that have been thermalized (i.e., decayed in the stable transporting levels) throughout diffusion across the emitting layer in the OLED.

### 4. Experimental Section

Experimental Details can be found in Supporting Information.

### Supporting Information

Supporting Information is available from the Wiley Online Library or from the author.

### Acknowledgements

This project has received funding from the European Union through the Interreg V initiative France-Wallonie-Vlaanderen—projet LUMINOPTX—and has been supported by the Belgian National Fund for Scientific Research (FRS-FNRS). Computational resources were provided by the Consortium des Équipements de Calcul Intensif (CÉCI) funded by F.R.S.-FNRS under Grant 2.5020.11. J.C. is an FNRS research director. C.P. thanks the ANR for financial support under the project SPIROQUEST (n°19-CE05-0024), the Region Bretagne (DIADEM), and the ADEME (EcoElec) for the Ph.D. grant and post-doctoral position (CB and FL resp.). Dr. Bruno Lafitte (ADEME), Rennes Metropole, and the CRMPO (Rennes) are also thanked. The authors thank Dr. J.-F. Bergamini (Rennes) for the TOC material. Y.O. acknowledges funding by the Fonds de la Recherche Scientifique-FNRS under Grant n° F.4534.21 (MIS-IMAGINE). The authors wish to thank Joëlle Rault Berthelot (Rennes) for the electrochemistry of SIA-2,7-F(POPh<sub>2</sub>)<sub>2</sub>.

### Conflict of Interest

The authors declare no conflict of interest.

### Data Availability Statement

The data that support the findings of this study are available from the corresponding author upon reasonable request.

### Keywords

density functional theory, electroluminescence, light emission, phosphine groups, spiro compounds

Received: May 4, 2022

Revised: June 27, 2022

Published online:

- [1] G. Hong, X. Gan, C. Leonhardt, Z. Zhang, J. Seibert, J. M. Busch, S. Bräse, *Adv. Mater.* **2021**, *33*, 2005630.
- [2] C. Poriel, J. Rault-Berthelot, *Adv. Funct. Mater.* **2020**, *30*, 1910040.
- [3] J. R. Sheats, H. Antoniadis, M. Hueschen, W. Leonard, J. Miller, R. Moon, D. Roitman, A. Stocking, *Science* **1996**, *273*, 884.
- [4] R. H. Friend, R. W. Gymer, A. B. Holmes, J. H. Burroughes, R. N. Marks, C. Taliani, D. D. C. Bradley, D. A. Dos Santos, J. L. Brédas, M. Lögdlund, W. R. Salaneck, *Nature* **1999**, *397*, 121.
- [5] M. A. Baldo, D. F. O'Brien, Y. You, A. Shoustikov, S. Sibley, M. E. Thompson, S. R. Forrest, *Nature* **1998**, *395*, 151.

- [6] Y. Tao, C. Yang, J. Qin, *Chem. Soc. Rev.* **2011**, *40*, 2943.
- [7] K. S. Yook, J. Y. Lee, *Adv. Mater.* **2014**, *26*, 4218.
- [8] C. Poriel, J. Rault-Berthelot, *J. Mater. Chem. C* **2017**, *5*, 3869.
- [9] C. Poriel, J. Rault-Berthelot, *Adv. Funct. Mater.* **2021**, *31*, 2010547.
- [10] Y. Wang, J. H. Yun, L. Wang, J. Y. Lee, *Adv. Funct. Mater.* **2021**, *31*, 2008232.
- [11] Q. Wang, F. Lucas, C. Quinton, Y. K. Qu, J. Rault-Berthelot, O. Jeannin, S. Y. Yang, F. C. Kong, S. Kumar, L. S. Liao, C. Poriel, Z. Q. Jiang, *Chem. Sci.* **2020**, *11*, 4887.
- [12] A. Endo, M. Ogasawara, A. Takahashi, D. Yokoyama, Y. Kato, C. Adachi, *Adv. Mater.* **2009**, *21*, 4802.
- [13] M. Y. Wong, E. Zysman-Colman, *Adv. Mater.* **2017**, *29*, 1605444.
- [14] C. Y. Chan, M. Tanaka, Y. T. Lee, Y. W. Wong, H. Nakanotani, T. Hatakeyama, C. Adachi, *Nat. Photonics*. **2021**, *15*, 203.
- [15] N. B. Kotadiya, P. W. M. Blom, G. J. A. H. Wetzelaer, *Nat. Photonics* **2019**, *13*, 765.
- [16] P. Tourneur, F. Lucas, C. Quinton, Y. Olivier, R. Lazzaroni, P. Viville, J. Cornil, C. Poriel, *J. Mater. Chem. C* **2020**, *8*, 14462.
- [17] F. Lucas, C. Quinton, S. Fall, T. Heiser, D. Tondelier, B. Geffroy, N. Leclerc, J. Rault-Berthelot, C. Poriel, *J. Mater. Chem. C* **2020**, *8*, 16354.
- [18] F. Lucas, O. A. Ibraikulov, C. Quinton, L. Sicard, T. Heiser, D. Tondelier, B. Geffroy, N. Leclerc, J. Rault-Berthelot, C. Poriel, *Adv. Opt. Mater.* **2020**, *8*, 1901225.
- [19] M. Romain, D. Tondelier, B. Geffroy, O. Jeannin, E. Jacques, J. Rault-Berthelot, C. Poriel, *Chem. Eur. J.* **2015**, *21*, 9426.
- [20] G. Méhes, H. Nomura, W. Zhang, T. Nakagawa, C. Adachi, *Angew. Chem. Int. Ed.* **2012**, *51*, 11311.
- [21] T. P. I. Saragi, T. Spehr, A. Siebert, T. Fuhrmann-Lieker, J. Salbeck, *Chem. Rev.* **2007**, *107*, 1011.
- [22] A. C. Morteani, A. S. Dhoot, J. S. Kim, C. Silva, N. Greenham, C. Murphy, E. Moons, S. Ciná, J. H. Burroughes, R. H. Friend, *Adv. Mater.* **2003**, *15*, 1708.
- [23] T. C. Lin, M. Sarma, Y. T. Chen, S. H. Liu, K. T. Lin, P. Y. Chiang, W. T. Chuang, Y. C. Liu, H. F. Hsu, W. Y. Hung, C. W. Tang, K. T. Wong, P. T. Chou, *Nat. Commun.* **2018**, *9*, 3111.
- [24] Y. Hong, J. W. Y. Lam, B. Z. Tang, *Chem. Soc. Rev.* **2011**, *40*, 5361.
- [25] F. Lucas, D. Tondelier, B. Geffroy, T. Heiser, O. A. Ibraikulov, C. Quinton, N. Leclerc, J. Rault-Berthelot, C. Poriel, *Mater. Chem. Front.* **2021**, *5*, 8066.
- [26] C. Poriel, J. Rault-Berthelot, S. Thiery, C. Quinton, O. Jeannin, U. Biapo, B. Geffroy, D. Tondelier, *Chem. Eur. J.* **2016**, *22*, 17930.
- [27] C. Quinton, L. Sicard, O. Jeannin, N. Vanthuyne, C. Poriel, *Adv. Funct. Mater.* **2018**, *28*, 180340.
- [28] S. Thiery, D. Tondelier, B. Geffroy, O. Jeannin, J. Rault-Berthelot, C. Poriel, *Chem. Eur. J.* **2016**, *22*, 10136.
- [29] Y. X. Zhang, L. Ding, X. Y. Liu, H. Chen, S. J. Ji, L. S. Liao, *Org. Electron.* **2015**, *20*, 112.
- [30] D. Zhang, W. Shen, H. Sun, R. He, M. Li, *ChemistrySelect* **2017**, *2*, 6604.
- [31] J. A. Seo, M. S. Gong, J. Y. Lee, *Org. Electron.* **2014**, *15*, 3773.
- [32] Y. Olivier, M. Moral, L. Muccioli, J. C. Sancho-García, *J. Mater. Chem. C* **2017**, *5*, 5718.
- [33] M. Moral, L. Muccioli, W. J. Son, Y. Olivier, J. C. Sancho-García, *J. Chem. Theor. Comput.* **2015**, *11*, 168.
- [34] T. Penfold, *J. Phys. Chem. C* **2015**, *119*, 13535.
- [35] H. Sun, C. Zhong, J. L. Brédas, *J. Chem. Theor. Comput.* **2015**, *11*, 3851.
- [36] A. Dreuw, M. Head-Gordon, *Chem. Rev.* **2005**, *105*, 4009.
- [37] T. Etienne, X. Assfeld, A. Monari, *J. Chem. Theor. Comput.* **2014**, *10*, 3896.
- [38] T. Etienne, X. Assfeld, A. Monari, *J. Chem. Theor. Comput.* **2014**, *10*, 3906.
- [39] Y. Olivier, B. Yurash, L. Muccioli, G. D'Avino, O. Mikhnenko, J. C. Sancho-García, C. Adachi, T. Q. Nguyen, D. Beljonne, *Phys. Rev. Mater.* **2017**, *1*, 075602.
- [40] H. Uoyama, K. Goushi, K. Shizu, H. Nomura, C. Adachi, *Nature* **2012**, *492*, 234.
- [41] G. D'Avino, S. Mothy, L. Muccioli, C. Zannoni, L. Wang, J. Cornil, D. Beljonne, F. Castet, *J. Phys. Chem. C* **2013**, *117*, 12981.
- [42] A. J. Gillett, C. Tonnelé, G. Londi, G. Ricci, M. Catherin, D. M. L. Unson, D. Casanova, F. Castet, Y. Olivier, W. M. Chen, E. Zaborova, E. W. Evans, B. H. Drummond, P. J. Conaghan, L. S. Cui, N. C. Greenham, Y. Puttisong, F. Fages, D. Beljonne, R. H. Friend, *Nat. Commun.* **2021**, *12*, 6640.